Inorganic Chemistry
Forum Article

Inorg. Chem. **2010**, *49*, 3557–3566 **3557**
DOI: 10.1021/ic9022486

Electroreduction of Dioxygen for Fuel-Cell Applications: Materials and Challenges

Andrew A. Gewirth* and Matthew S. Thorum

Department of Chemistry, University of Illinois at Urbana−Champaign, Urbana, Illinois 61801

Received November 13, 2009

A review of the oxygen reduction reaction (ORR) and its use in fuel-cell applications is presented. Discussed are mechanisms of the ORR and implementations of catalysts for this reaction. Specific catalysts discussed include nanoparticles, macrocycles and pyrolysis products, carbons, chalcogenides, enzymes, and coordination complexes. A prospectus for future efforts is provided.

1. Introduction

The activation of dioxygen is important in contexts ranging from biology to materials dissolution. One area seeing renewed focus is the oxygen reduction reaction (ORR) and its role in fuel cells.[1−4] A fuel cell[5] is an electrochemical device that generates electricity through the spatially separated oxidation of a fuel and the reduction of an oxidant, typically dioxygen. A schematic of a fuel cell is shown in Figure 1.

A fuel cell consists of two electrodes separated by an electrolyte or membrane. At one electrode, the anode, a fuel is oxidized. Typical fuels include hydrogen, methanol, ethanol, or formic acid. Of these, only the first two are easily oxidized using present day catalysts, which are typically platinum-based.[6] For hydrogen fuel, the half-reaction is

$$H_2(g, 1\ atm) \rightarrow 2H^+(aq, 1\ M) + 2e^-, \quad E^0 = 0.0\ V \quad (1)$$

The electrocatalysis of methanol or ethanol oxidation at an electrode surface is a subject unto itself and the focus of intense study, if not great progress, over the last 40 years.[4,7]

At the other electrode, the cathode, a reduction must occur to ensure electroneutrality of the fuel cell. Regardless of the fuel, the species to be reduced is almost always dioxygen. Desired is the four-electron reduction of dioxygen to water, the ORR:

$$O_2(g, 1\ atm) + 4e^- + 4H^+(aq, 1\ M) \rightarrow 2H_2O, \quad E^\circ = 1.23\ V \quad (2)$$

The combined reaction then is

$$H_2 + \frac{1}{2}O_2 \rightarrow H_2O, \quad \Delta E = 1.23\ V \quad (3)$$

The first half-reaction, involving hydrogen oxidation, is facile with present day platinum-based catalysts. However, the ORR is not facile, even with a platinum catalyst. The difficulty in oxygen reduction stems from the exceptionally strong O═O bond (498 kJ/mol). Thus, activation of this bond is typically kinetically slow.

At both the anode and cathode, the catalyst is supported on carbon usually found as a felt onto which the catalyst has been impregnated. The separator between the two electrodes is a polymer electrolyte now commonly made from the conductive fluoropolymer Nafion. The combined polymer electrode assembly is known as a membrane electrode assembly (MEA).

There several different types of fuel cells, ranging from the high-temperature solid oxide fuel cell (SOFC) to the lower temperature operating polymer electrolyte membrane (PEM) fuel cell.[5] For space applications, alkaline fuel cells have been utilized, but the presence of CO_2 in the terrestrial atmosphere means that insoluble carbonates will be present in any basic pH implementation. These insoluble carbonates will ultimately poison the fuel cell.[8] High-pH (pH > 12) fuel cells also have intrinsically slower H_2 oxidation kinetics.[9]

*To whom correspondence should be addressed. E-mail: agewirth@illinois.edu. Tel: 217-333-8329. Fax: 217-244-3186.

(1) Markovic, N. M.; Schmidt, T. J.; Stamenkovic, V.; Ross, P. N. *Fuel Cells* **2001**, *1*, 105–116.
(2) Markovic, N. M.; Ross, P. N. In *Interfacial Electrochemistry*; Wieckowski, A., Ed.; Marcel Dekker: New York, 1999; pp 821−841.
(3) Adzic, R. In *Electrocatalysis*; Lipkowski, J., Ross, P. N., Eds.; Wiley-VCH, Inc.: New York, 1998; pp 197−242.
(4) Vielstich, W.; Lamm, A.; Gasteiger, H. *Handbook of Fuel Cells: Fundamentals, Technology, Applications*; John Wiley and Sons: Chichester, U.K., 2003.
(5) Dresselhaus, M.; Crabtree, G.; Buchanan, M. *Basic Research Needs for the Hydrogen Economy*; U.S. Department of Energy: Washington, DC, 2003.
(6) Borup, R.; Meyers, J.; Pivovar, B.; Kim, Y. S.; Mukundan, R.; Garland, N.; Myers, D.; Wilson, M.; Garzon, F.; Wood, D.; Zelenay, P.; More, K.; Stroh, K.; Zawodzinski, T.; Boncella, J.; McGrath, J. E.; Inaba, M.; Miyatake, K.; Hori, M.; Ota, K.; Ogumi, Z.; Miyata, S.; Nishikata, A.; Siroma, Z.; Uchimoto, Y.; Yasuda, K.; Kimijima, K. I.; Iwashita, N. *Chem. Rev.* **2007**, *107*, 3904–3951.
(7) Antolini, E.; Lopes, T.; Gonzalez, E. R. *J. Alloys Compd.* **2008**, *461*, 253–262.
(8) Tewari, A.; Sambhy, V.; Macdonald, M. U.; Sen, A. *J. Power Sources* **2006**, *153*, 1–10.
(9) Cabot, P. L.; Alcaide, F.; Brillas, E. *J. Electroanal. Chem.* **2009**, *626*, 183–191.

Published on Web 04/12/2010

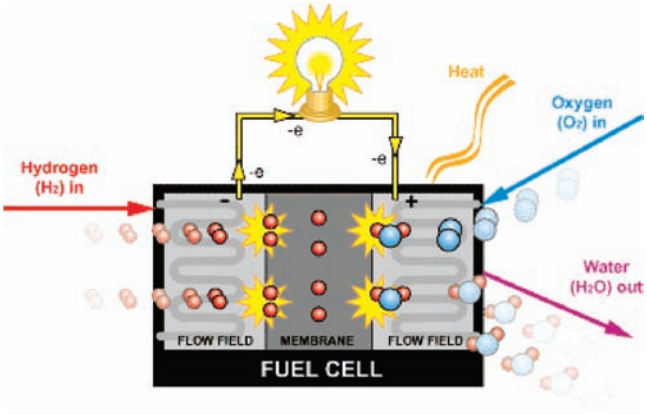

Figure 1. Schematic of a hydrogen/air fuel cell. Hydrogen is oxidized at the anode (left), and protons travel across the membrane to the cathode (right) where oxygen is reduced to water. Reprinted with permission from ref 5. Copyright U.S. Department of Energy 2003.

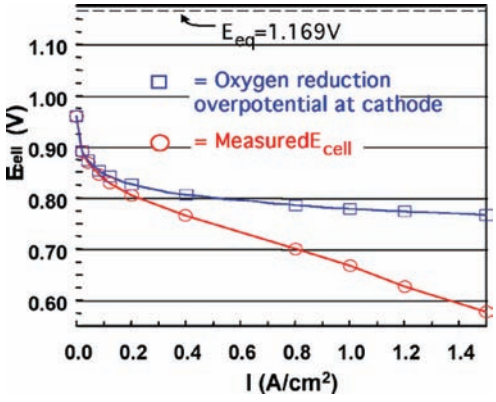

Figure 2. Plot of the cell voltage as a function of the current for a hydrogen/air fuel cell showing the substantial drop in the cell voltage at higher currents. This drop is related to diminished thermodynamic efficiency.[5]

Thus, there is a substantial effort directed at low- (pH < 2) and intermediate-pH fuel cell devices, particularly for automotive applications. Applications for low-power devices, such as cell phones and portable computers, might utilize formic acid or methanol as a fuel, in addition to H_2. However, the cathode in these applications still utilizes dioxygen and the ORR.

The single most important attraction of fuel cells relates to their potential for highly efficient use of a fuel, particularly for transportation applications. Because the fuel cell is not a heat engine, the Carnot cycle laws, which place limits on the thermodynamic efficiency of these devices, do not apply. For example, burning H_2 in an internal combustion engine has a thermodynamic efficiency of ca. 10−20%.[4] By way of contrast, the theoretical thermodynamic efficiency of a hydrogen-utilizing fuel cell is nearly 93% at 25 °C and other fuels have greater values.[10,11] Unfortunately, numbers like these are not realized in practical installations, and the best efficiencies, found in automotive fuel cells, are on the order of 45−50%. Of course, these numbers do not include the energy required to compress the hydrogen for storage on the vehicle or the energy spent in generating the hydrogen itself. "Well-to-wheel" numbers for fuel-cell efficiency are typically in the 30% region.[4]

The ultimate vision for a sustainable future would involve the utilization of hydrogen generated through electrolysis of water using solar energy in a fuel cell. In this way, the dependence on dwindling oil supplies or on coal liquefaction might be eliminated. The use of hydrogen would have a positive impact on the generation of atmospheric carbon dioxide.

The focus of this review is on the electroreduction of oxygen in an acid environment, a crucial component in fuel-cell systems. The major reason that present day low-temperature fuel cells do not exhibit their theoretical thermodynamic efficiencies is related to the ORR. Since the early 1960s, investigators recognized that the slow kinetics of the ORR in an acid solution present a major impediment for fuel-cell development and the importance of this subject has been recognized in a number of reviews over the years.[12−16]

The slow kinetics of the ORR gives rise to the now nearly canonical overpotential/current curves shown in Figure 2. Figure 2 is a plot of the cell potential versus current for a hydrogen/air fuel cell. The cell potential is the difference between the potentials of two half cells—one $H_2/2H^+$ defined at 0.0 V and the other the ORR at +1.23 V (1.169 V with the lower activity of dioxygen in air at 80 °C)—so that the theoretical difference is 1.23 V. The figure shows that substantial currents cannot be obtained with cell voltages anywhere near the thermodynamic value of 1.23 V. Indeed, there is little current observed until the cell voltage drops below 1.0 V. Instead, more driving force or overpotential is required to achieve these reasonable currents, with required currents being on the order of ca. 1.5 A/cm^2 of electrode material. The figure shows that only about 50% of the thermodynamic voltage is obtained with these larger currents.

There is a direct relationship between the cell overpotential and fuel-cell electrical efficiency, ζ, as given in eq 4.[17]

$$\zeta = 1 - \frac{\eta_a + \eta_c}{\Delta E^\circ} \tag{4}$$

where η_a and η_c are the overpotentials at the anode and cathode, respectively, and ΔE° is the total cell potential. For the case of the hydrogen/oxygen fuel cells, η_a is on the order of 50 mV, while η_c is 500−600 mV (e.g., for a fuel cell running at 80 °C and 1.5 A/cm^2 of the assembly area).[18] With E° = 1.23 V, ζ = 55−45%, depending on the exact value of η_c. This value means that, even before questions regarding the production and storage of H_2 are addressed, the best efficiency obtainable with current catalyst packages is quite low (ca. 40%) relative to theoretical values. This low

(10) Lutz, A. E.; Larson, R. S.; Keller, J. O. *Int. J. Hydrogen Energy* **2002**, *27*, 1103–1111.
(11) Kartha, S.; Grimes, P. *Phys. Today* **1994**, *47*, 54–61.
(12) Damjanovic, A. In *Electrochem. Transition*; Murphy, O. J., Srinivasan, S., Conway, B. E., Eds.; Plenum Press: New York, 1992; pp 107−126.
(13) Appleby, A. J. *J. Electroanal. Chem.* **1993**, *357*, 117–179.
(14) Srinivasan, S.; Dave, B. B.; Murugesamoorthi, K. A.; Parthasarathy, A.; Appleby, A. J. *Fuel Cell Syst.* **1993**, 37–72.
(15) Damjanovic, A. In *Modern Aspects of Electrochemistry*; Conway, B. E., Bockris, J. O., Eds.; Plenum Press: New York, 1969; Vol. *5*, pp 369−483.
(16) Tarasevich, M. R.; Sadkowski, A.; Yeager, E. In *Comprehensive Treatise of Electrochemistry*; Conway, B. E., Bockris, J. O. M., Yeager, E., Kahn, S. U. M., White, R. E., Eds.; Plenum: New York, 1983; Vol. *7*, pp 301−398.
(17) Jarvi, T. D.; Stuve, E. M. *Electrocatalysis* **1998**, 75–133.
(18) Gasteiger, H. A.; Panels, J. E.; Yan, S. G. *J. Power Sources* **2004**, *127*, 162–171.

efficiency obviates much of the intrinsic attraction of the fuel cell for transportation applications.

One way to get around the relatively high overpotentials of the ORR is to use more catalyst and move to lower overpotentials (less driving force), giving rise to fewer turnovers per site per second but overall larger currents through increases in the total sites. In order to support realistic cell currents, relatively high platinum loadings have been used.[18] The intrinsic cost of these materials, dependent on elemental availability and market forces, means that catalyst costs can be quite expensive, in the $5000−10000 range.[18] These numbers alone provide a substantial impediment to fuel-cell usage.

The ORR on platinum in acid usually proceeds via a four-electron process. However, occasionally—from 2% to 0.01% of the time depending on conditions—some of the oxygen is reduced only to hydrogen peroxide.[19] The origin of the peroxide is still somewhat controversial, with explanations ranging from contaminated Pt sites to reduced retention time for peroxide intermediates.[20] Peroxide generation has a number of negative consequences. For example, peroxide generation is associated with catalyst instability, and at long times (ca. 5000 h of operation) platinum-based catalyst particles exhibit agglomeration and dissolution into the membrane, which further depolarizes the cell, and yield even lower efficiencies.[21,22] Even worse, the peroxide decomposes the commonly used Nafion separator/electrolyte material.

A further issue regarding the platinum-based ORR catalyst has to do with diffusion of fuel across the membrane either during or after fuel-cell activity. In the former, this "crossover" phenomenon can lead to electrode fouling particularly when the fuel contains carbon. Additionally, the presence of an oxidation event at the fuel-cell cathode leads to cell depolarization and further drops in efficiency. The use of a catalyst selective for only the ORR would ameliorate this issue.

With the understanding of the direct implications of the slow ORR kinetics on thermodynamic efficiency, fuel-cell stability, and catalyst cost has come a dramatic increase in research activity on all aspects of the ORR. This activity is divided into several phases. In the following, we discuss work directed at understanding the mechanism of the ORR on transition-metal surfaces. We then discuss potential new catalysts for ORR fuel-cell implementations. In this review, we focus particularly on the ORR in acid or neutral environments because it is at these pHs that terrestrial applications of the fuel cell will likely see implementation. Finally, we close with a prospectus.

2. Mechanisms of the ORR

The mechanisms associated with the ORR have been a subject of investigation for several decades, particularly as they relate to platinum. These efforts have both an experimental and a theoretical component. Early work by Yeager and colleagues with observables based largely on a rotating-ring disk electrode (RRDE) and current versus overpotential (Tafel slope) considerations led to a proposed model of sequential reduction through various surface-bound intermediates,[16,23,24] as shown in Figure 3.

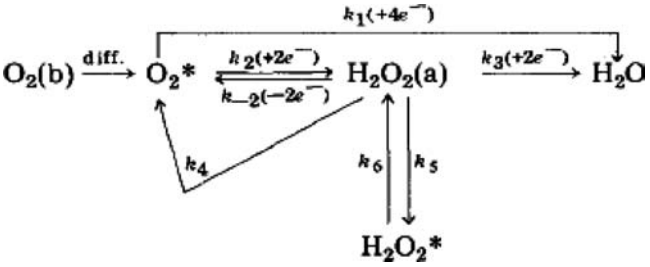

Figure 3. Cannonical mechanism for the ORR in an acid solution showing both direct and series pathways. O_2(b) is oxygen in solution. O_2* is electrode-surface-associated oxygen.[23]

Here, two different processes are putatively operative. First, the "direct" mechanism (k_1) sees a concerted four-electron transfer, reducing dioxygen to water. Second, the "series" mechanism features a series of one- or two-electron transfers yielding possibly transient superoxo (not shown) and peroxo surface species. Discrimination between the two pathways, and indeed discrimination between generally associative and dissociative mechanisms of dioxygen reactivity on platinum in the aqueous electrochemical environment, has occupied the community for the past several decades.[25]

The ORR on platinum proceeds via a four-electron direct process nearly all of the time, with a small amount (ca. 1%) of peroxide formed at low (100−400 mV) overpotentials. On other surfaces, such as gold, the ORR proceeds via a two-electron reduction to peroxide at relatively low overpotentials in acid. However, in the basic electrochemical environment, some low Miller index faces of gold [Au(100)] exhibit four-electron reduction of dioxygen, while others do not.[26,27]

Experimental investigations of the ORR on platinum take the form of electrochemical, synthetic, and spectroscopic studies. Long ago, researchers noted that plots of the log of the ORR current, i, as a function of the overpotential η (the Tafel plot, a type of linear free-energy plot[28]) exhibited two slopes. One Tafel slope at high currents (and high overpotentials) has a value of 120 mV/decade, while the other at lower currents (and lower overpotentials) has a value of 60 mV/decade. The presence of these two slopes implies that two different mechanisms are operative for the ORR at different overpotentials. The 120 mV/decade Tafel slope is interpreted as suggesting that the first electron transfer is rate-limiting.[3] In both potential regimes, the ORR is found to be first-order in [O_2]. The reactivity in the low overpotential region may be controlled by adsorbed anions (or more specifically, the desorption of adsorbed anions).[29,30] More recently, there is

(19) Bonakdarpour, A.; Dahn, T. R.; Atanasoski, R. T.; Debe, M. K.; Dahn, J. R. *Electrochem. Solid State Lett.* **2008**, *11*, B208–B211.
(20) Seidel, Y. E.; Schneider, A.; Jusys, Z.; Wickman, B.; Kasemo, B.; Behm, R. J. *Faraday Discuss.* **2008**, *140*, 167–184.
(21) Shao-Horn, Y.; Sheng, W. C.; Chen, S.; Ferreira, P. J.; Holby, E. F.; Morgan, D. *Top. Catal.* **2007**, *46*, 285–305.
(22) Ferreira, P. J.; la O, G. J.; Shao-Horn, Y.; Morgan, D.; Makharia, R.; Kocha, S.; Gasteiger, H. A. *J. Electrochem. Soc.* **2005**, *152*, A2256–A2271.
(23) Wroblowa, H. S.; Pan, Y. C.; Razumney, G. *J. Electroanal. Chem.* **1976**, *69*, 195–201.
(24) Yeager, E. *Electrochim. Acta* **1984**, *29*, 1527–1537.
(25) Wang, J. X.; Zhang, J. L.; Adzic, R. R. *J. Phys. Chem. A* **2007**, *111*, 12702–12710.
(26) Adzic, R. R.; Markovic, N. M.; Vesovic, V. B. *J. Electroanal. Chem.* **1984**, *165*, 105–120.
(27) Strbac, S.; Adzic, R. R. *Electrochim. Acta* **1996**, *41*, 2903–2908.
(28) Bard, A. J.; Faulkner, L. R. *Electrochemical Methods: Fundamentals and Applications*; 2nd ed.; John Wiley & Sons, Inc.: New York, 2001.
(29) Wang, J. X.; Markovic, N. M.; Adzic, R. R. *J. Phys. Chem. B* **2004**, *108*, 4127–4133.
(30) Stamenkovic, V.; Markovic, N. M.; Ross, P. N. *J. Electroanal. Chem.* **2001**, *500*, 44–51.

a growing consensus that the different Tafel slopes are associated with different potential-dependent OH^- coverages on the platinum surface. A high-coverage region at low overpotentials gives a low Tafel slope, and a low-OH-coverage region at lower potentials gives a higher Tafel slope.[31,32]

Even at this relatively late date, there still is no consensus concerning the primary steps of the ORR on platinum or indeed any other surface. On platinum, both associative and dissociative mechanisms have been proposed. In the former, dioxygen binds to a metal surface and then transforms to a bound superoxide following the first electron transfer with a possible coupled proton transfer. In the latter, dioxygen dissociates upon platinum coordination, a process similar to what occurs during dioxygen association with platinum under ultrahigh-vacuum (UHV) conditions in the absence of electrolyte and applied potential.[34] Observation of intermediates in the ORR could help confirm or disprove a specific mechanism, but these have been elusive.

On the basis of poisoning studies, there is an emerging consensus that the ORR proceeds by using at least two Pt atoms on the platinum surface, with end-on coordination to one Pt at very high overpotentials in the dihydrogen region responsible for a further shift to a two-electron mechanism.[1] Observation of a bound peroxide or superoxide could confirm the associative mechanism, but definitive observation of this species in the acid electrochemical environment has been obtained only for the bismuth underpotential deposition (upd)[35] system.[36]

On surfaces other than platinum, there is also considerable ambiguity regarding the mechanism of the ORR. On certain surfaces, such as those formed by the upd of bismuth on Au(111), spectroscopic studies reveal the presence of a bound surface hydroxide during the course of the two-electron reduction of peroxide[33] and a bound superoxide[36] formed during the course of the four-electron reduction of oxygen. Figure 4 shows a proposed reaction pathway for peroxide reduction on a bismuth-modified Au(111) surface.[33]

A bound surface hydroxide was also observed as a consequence of peroxide reduction on many other surfaces, such as those formed by the upd of lead on Au(111),[37] copper,[38] gold,[39] and even platinum.[40] These experimental studies, along with corresponding calculations, suggest that cleavage of the O−O bond on these surfaces occurs at the peroxide oxidation state level. On nonmetallic surfaces, there remains considerable uncertainty regarding the nature of the active site, and this ambiguity precludes the development of mechanistic understanding.

An alternative mechanism to the ORR argues that O−O bond cleavage occurs at the level of dioxygen association to the metal surface, as is found in the UHV environment on

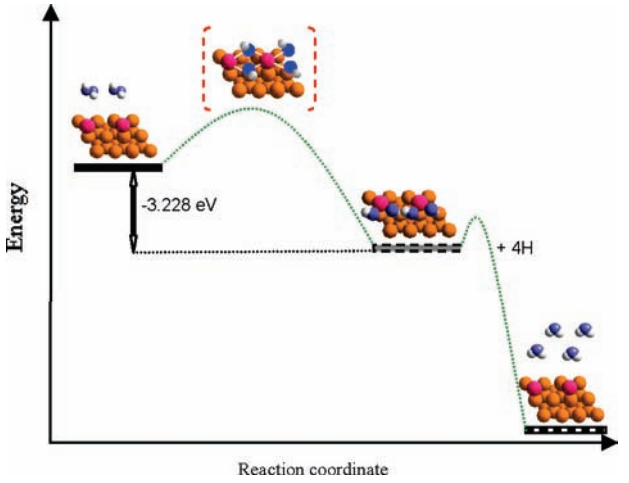

Figure 4. Proposed hydrogen peroxide reduction mechanism on the 2×2 Bi/Au(111) surface. The structure enclosed in red brackets is an intermediate not calculated in this work. The orange, pink, blue, and white circles represent the Au, Bi, O, and H atoms, respectively.[33]

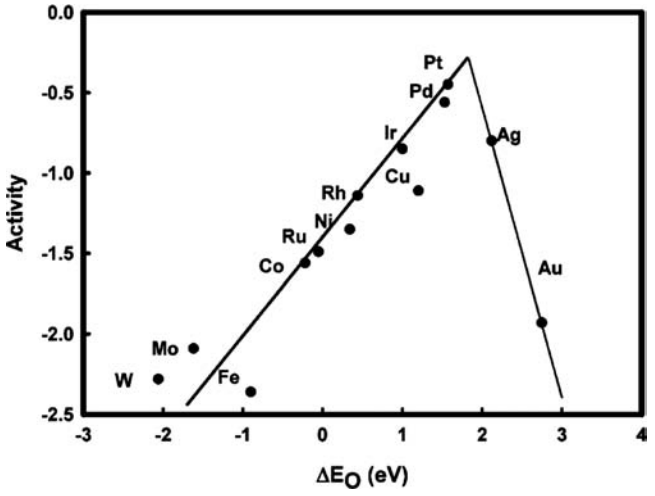

Figure 5. Trends in oxygen reduction activity plotted as a function of the oxygen binding energy. Reprinted from ref 45.

platinum. This idea forms the basis for a combinatorial exploration of different catalysts,[41,42] as well as theory.[43,44]

One particularly successful approach to elucidating ORR kinetics on metal surfaces has been through the agency of the "d-band model" popularized by Norskov and co-workers and later used as the foundational basis for new catalyst design by several groups. This model involves the coupling of adsorbate states with metal d states on the electrode. By examination of the strength of coupling between O, O_2, or OH on different metals, so-called "volcano plots" relating this strength to reactivity can be developed. These plots are a manifestation of the principle of Sabatier, well-known in the heterogeneous catalysis literature.[34] Figure 5,[45] shows one of

(31) Tian, F.; Jinnouchi, R.; Anderson, A. B. *J. Phys. Chem. C* **2009**, *113*, 17484–17492.
(32) Rai, V.; Aryanpour, M.; Pitsch, H. *J. Phys. Chem. C* **2008**, *112*, 9760–9768.
(33) Li, X.; Gewirth, A. A. *J. Am. Chem. Soc.* **2003**, *125*, 7086–7099.
(34) Masel, R. I. *Principles of Adsorption and Reaction on Solid Surfaces*; Wiley: New York, 1995.
(35) Adzic, R. R. In *Advances in Electrochemistry and Electrochemical Engineering*; Gerischer, H., Tobias, C. W., Eds.; Wiley-Interscience: New York, 1984; Vol. *13*, pp 159−260.
(36) Li, X.; Gewirth, A. A. *J. Am. Chem. Soc.* **2005**, *127*, 5252–5260.
(37) Li, X.; Gewirth, A. A. *J. Raman Spectrosc.* **2005**, *36*, 715–724.
(38) Stewart, K. L.; Gewirth, A. A. *Langmuir* **2007**, *23*, 9911–9918.
(39) Kim, J. W.; Gewirth, A. A. *J. Phys. Chem. B* **2006**, *110*, 2565–2571.
(40) Li, X.; Heryadi, D.; Gewirth, A. A. *Langmuir* **2005**, *21*, 9251–9259.
(41) Walsh, D. A.; Fernandez, J. L.; Bard, A. J. *J. Electrochem. Soc.* **2006**, *153*, E99–E103.
(42) Fernandez, J. L.; Walsh, D. A.; Bard, A. J. *J. Am. Chem. Soc.* **2005**, *127*, 357–365.
(43) Wang, J. X.; Uribe, F. A.; Springer, T. E.; Zhang, J. L.; Adzic, R. R. *Faraday Discuss.* **2008**, *140*, 347–362.
(44) Rossmeisl, J.; Karlberg, G. S.; Jaramillo, T.; Norskov, J. K. *Faraday Discuss.* **2008**, *140*, 337–346.
(45) Norskov, J. K.; Rossmeisl, J.; Logadottir, A.; Lindqvist, L.; Kitchin, J. R.; Bligaard, T.; Jonsson, H. *J. Phys. Chem. B* **2004**, *108*, 17886–17892.

these plots, which shows that among pure metals platinum has the highest reactivity. The strength of coupling between O or OH and the metal surface can also be changed by alloying. Markovic and co-workers used this idea to show that there was an excellent correlation between the strength of coupling as determined using the d-band model and experimental ORR rates,[46] a result confirmed by other groups.[47] In particular, the rates of reactivity can be controlled by controlling the position of this d band by the appropriate construction of nanoparticles.[46] One triumph of this approach is the recent report by Markovic and co-workers showing high rates (low overpotentials) on Pt/Ni, where the reactivity of the first layer, platinum, is altered by a second layer enriched in nickel.[48] This reactivity, found in well-defined single crystals, has not yet been replicated in small particles that would be required for fuel-cell applications. A corresponding theoretical effort enabled by many groups surrounds this effort.[49,50]

3. Nanoparticles

3.1. Platinum. Metallic platinum has been the oxygen reduction catalyst of choice since the development of the PEM fuel cell by General Electric in the early 1960s, and it remains the benchmark against which the activities of all new ORR catalysts are evaluated.[51,52] Because the scarcity and cost of platinum are significant barriers to the commercialization of the PEM fuel cell, intensive research efforts have focused on reducing the platinum catalyst loading while maintaining cell potentials. Unfortunately, simply reducing the amount of catalyst applied to the electrode generally results in significant reductions in the cell voltage and power density.

Currently, state-of-the-art PEM fuel cell cathodes have platinum loadings of ca. 0.4 mg_{Pt}/cm^2 and demonstrate mass activities of ca. 0.16 A/mg_{Pt} at 0.9 V vs RHE (V_{RHE}); a reduction of the platinum loading to 0.15 mg_{Pt}/cm^2 (corresponding to a target mass activity of ca. 0.45 A/mg_{Pt} at 0.9 V_{RHE}) is required for large-scale automotive applications.[51] These catalysts generally consist of ~40% Pt/C in the form of carbon-black-supported platinum nanoparticles with diameters of ca. 3−4 nm and active surface areas of ca. 90 m^2_{Pt}/g. "State-of-the-art" platinum catalysts are frequently reported in the literature with significantly lower activities than the above figures, and activities reported as "*x* times higher than platinum" should be treated with caution; actual specific or mass activities at 0.9 V_{RHE} are a superior basis for the comparison of platinum catalysts.

Catalysts with sub-3-nm platinum nanoparticles and increased active surface areas do not have increased mass activities over the state-of-the-art commercial catalysts. This is due to a size-dependent decrease in the ORR activity on platinum nanoparticles, which is attributed to the increasing adsorption strength of OH_{ads} species, which block active sites.[51−56]

Another attempt to reduce the platinum loading has been to prepare platinum nanoparticles with designer morphologies including various polyhedra, nanowires, and branched structures.[57−65] While some of these structures exhibit higher specific activities than 40% Pt/C, these improvements are more than compensated for by the reduced surface areas of these materials, resulting in no net gain in mass activities.[58]

Given these observations, it is not likely that the target mass activities can be reached with a pure platinum catalyst. This problem is compounded by the fact that the platinum catalysts gradually degrade upon potential cycling (via sintering, dissolution, and corrosion of the carbon support) and lack the durability required for automotive applications.[4]

Platinum Alloys. During the 1990s, researchers working on phosphoric acid electrolyte fuel cells (PAFCs) found that numerous binary and ternary platinum alloys exhibited higher ORR activity and greater stability than pure platinum. A variety of explanations have been invoked to explain the enhanced activities of various alloy catalysts including structural and electronic factors, and this early work has been reviewed previously.[51] Other reviews have addressed the growth mechanisms and structure of platinum alloy nanoparticles.[57,66] The base metal gradually leaches out of these catalysts, which is not a major concern in PAFCs; however, in PEM fuel cells, the leached cations poison the ionomer membrane (by displacing protonic sites) and catalyze the degradation of the membrane.[51,67] Preleaching Pt_xCo_{1-x} alloys with acid can prevent further leaching and contamination of the membrane electrode. Activity as high as 0.28 A/mg_{Pt} at 0.9 V_{RHE} reported using commercially available materials may be regarded as a benchmark for alloy catalysts.[51,68]

(46) Stamenkovic, V.; Mun, B. S.; Mayrhofer, K. J. J.; Ross, P. N.; Markovic, N. M.; Rossmeisl, J.; Greeley, J.; Norskov, J. K. *Angew. Chem., Int. Ed.* **2006**, *45*, 2897–2901.
(47) Lima, F. H. B.; Zhang, J.; Shao, M. H.; Sasaki, K.; Vukmirovic, M. B.; Ticianelli, E. A.; Adzic, R. R. *J. Phys. Chem. C* **2007**, *111*, 404–410.
(48) Stamenkovic, V. R.; Fowler, B.; Mun, B. S.; Wang, G. F.; Ross, P. N.; Lucas, C. A.; Markovic, N. M. *Science* **2007**, *315*, 493–497.
(49) Zhang, J. L.; Vukmirovic, M. B.; Xu, Y.; Mavrikakis, M.; Adzic, R. R. *Angew. Chem., Int. Ed.* **2005**, *44*, 2132–2135.
(50) Xu, Y.; Ruban, A. V.; Mavrikakis, M. *J. Am. Chem. Soc.* **2004**, *126*, 4717–4725.
(51) Gasteiger, H. A.; Kocha, S. S.; Sompalli, B.; Wagner, F. T. *Appl. Catal., B* **2005**, *56*, 9–35.
(52) Mayrhofer, K. J. J.; Strmcnik, D.; Blizanac, B. B.; Stamenkovic, V.; Arenz, M.; Markovic, N. M. *Electrochim. Acta* **2008**, *53*, 3181–3188.
(53) Mayrhofer, K. J. J.; Blizanac, B. B.; Arenz, M.; Stamenkovic, V. R.; Ross, P. N.; Markovic, N. M. *J. Phys. Chem. B* **2005**, *109*, 14433–14440.
(54) Yamamoto, K.; Imaoka, T.; Chun, W.-J.; Enoki, O.; Katoh, H.; Takenaga, M.; Sonoi, A. *Nat. Chem.* **2009**, advanced online publication.
(55) Ye, H.; Crooks, J. A.; Crooks, R. M. *Langmuir* **2007**, *23*, 11901–11906.
(56) Antoine, O.; Bultel, Y.; Durand, R. *J. Electroanal. Chem.* **2001**, *499*, 85–94.
(57) Peng, Z. M.; Yang, H. *Nano Today* **2009**, *4*, 143–164.
(58) Chen, J. Y.; Lim, B.; Lee, E. P.; Xia, Y. N. *Nano Today* **2009**, *4*, 81–95.
(59) Zhou, H. J.; Zhou, W. P.; Adzic, R. R.; Wong, S. S. *J. Phys. Chem. C* **2009**, *113*, 5460–5466.
(60) Shuhui, S.; Frédéric, J.; Jean-Pol, D. *Adv. Mater.* **2008**, *20*, 3900–3904.
(61) Wang, C.; Daimon, H.; Lee, Y.; Kim, J.; Sun, S. *J. Am. Chem. Soc.* **2007**, *129*, 6974.
(62) Cui, G. L.; Zhi, L. J.; Thomas, A.; Kolb, U.; Lieberwirth, I.; Mullen, K. *Angew. Chem., Int. Ed.* **2007**, *46*, 3464–3467.
(63) Wang, L.; Yamauchi, Y. *Chem. Mater.* **2009**, in press.
(64) Ye, H.; Crooks, R. M. *J. Am. Chem. Soc.* **2005**, *127*, 4930–4934.
(65) Chen, H. M.; Liu, R.-S.; Lo, M.-Y.; Chang, S.-C.; Tsai, L.-D.; Peng, Y.-M.; Lee, J.-F. *J. Phys. Chem. C* **2008**, *112*, 7522–7526.
(66) Zhong, C. J.; Luo, J.; Njoki, P. N.; Mott, D.; Wanjala, B.; Loukrakpam, R.; Lim, S.; Wang, L.; Fang, B.; Xu, Z. C. *Energy Environ. Sci.* **2008**, *1*, 454–466.
(67) Paulus, U. A.; Wokaun, A.; Scherer, G. G.; Schmidt, T. J.; Stamenkovic, V.; Radmilovic, V.; Markovic, N. M.; Ross, P. N. *J. Phys. Chem. B* **2002**, *106*, 4181–4191.
(68) Chen, S.; Ferreira, P. J.; Sheng, W.; Yabuuchi, N.; Allard, L. F.; Shao-Horn, Y. *J. Am. Chem. Soc.* **2008**, *130*, 13818–13819.

The most recent and promising advancements utilize various strategies to control the morphology of the nanoparticles and form heterogeneous structures including platinum skins and nanoparticles decorated with smaller particles or dendritic structures.

Palladium nanocrystals have been used as a seed for the formation of dendritic platinum nanoparticles upon reduction of platinum salts with ascorbic acid in an aqueous solution.[69] This technique is appealing because it is amenable to large-scale production. Even though the palladium seeds were relatively large (9 nm) compared to the typical Pt/C, the high surface area of the dendritic structures and the high activity of the platinum surfaces yields platinum mass activities as high as 0.43 A/mg_{Pt} at 0.9 V_{RHE}.[69] This activity approaches the activity targets for applications; however, this value does not take into account the palladium loading. The durability was found to be slightly better than Pt/C but still insufficient for practical applications. The use of smaller particles may allow further reductions in the noble metal loading if high activity can be maintained. A separate investigation found that 3 nm platinum nanoparticles grown on the surface of 5 nm palladium particles have relatively high activity compared to platinum (unfortunately, the actual mass activity was not reported) and good durability (ca. 12% decay after 30 000 potential cycles compared to a 39% decay in similarly treated platinum).[70]

The deposition of small gold clusters onto a Pt/C catalyst was shown to dramatically improve its durability without a significant decrease in the initial activity, proving that platinum-based materials may be prepared with sufficient durability for automotive application. The gold clusters were formed by galvanic displacement of a copper monolayer formed by upd followed by potential cycling, which is not amenable to large-scale production. The stabilization mechanism remains unclear.[71]

Enhancement of the ORR activity of Pt_3M alloys (M = Ni, Co, Fe, V, Ti) over pure platinum has been demonstrated on extended polyelectrodes and single-crystal electrodes that have been annealed, resulting in the formation of a monolayer platinum skin on the surface of the alloy.[48,72] In particular, the $Pt_3Ni(111)$ surface is approximately 10-fold more active than Pt(111)—90-fold more active than platinum nanoparticles on a mass activity basis—and has the highest ORR activity of any alloy reported to date (Figure 6). The enhancement is attributed to a negative shift in the d-band center that weakens the interaction of adsorbed intermediates with the surface, increasing the number of active sites for dioxygen adsorption.[48] Although this thermal annealing technique has produced impressive results on bulk surfaces, an extension to carbon-supported nanocatalysts is lacking.

A second method for producing a platinum skin on another metal is by the electrochemical upd of a monolayer of copper onto the metal followed by galvanic displacement of copper with platinum. This technique limits the underlaying metal to late transition metals such as palladium, gold, ruthenium, iridium, and rhodium; however, it can be extended to carbon-supported nanoparticles. The ORR mass activity of these platinum monolayer catalysts on both extended surfaces and nanoparticles has been demonstrated to be up to 20 times greater than that of platinum particles.[49,73−77] However,

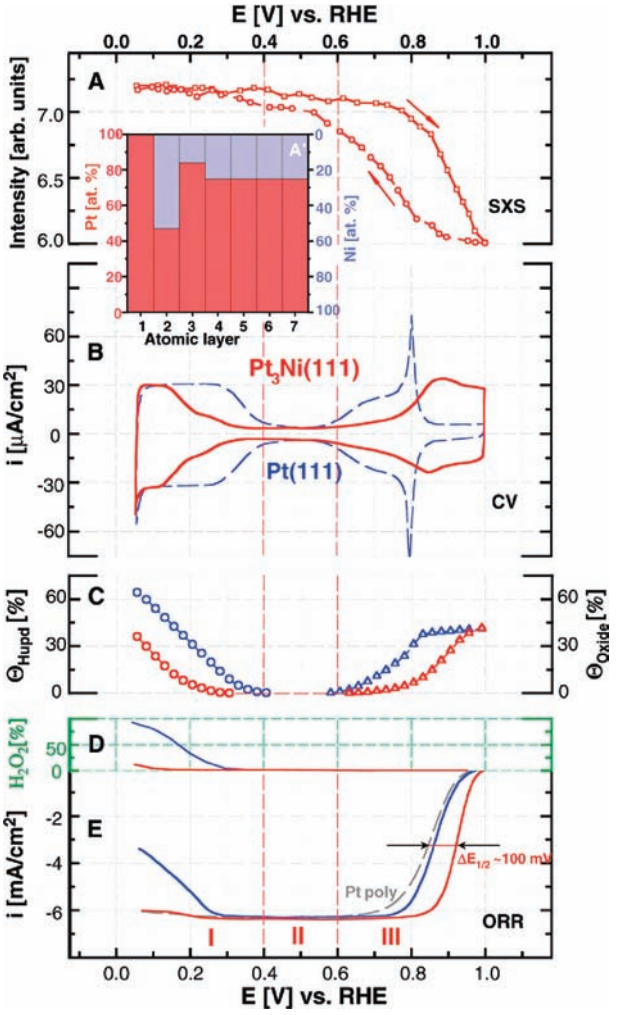

Figure 6. In situ characterization of the $Pt_3Ni(111)$ surface in $HClO_4$ (0.1 M) at 333 K. (A) Small-angle X-ray scattering (SAXS) data and (A′) concentration profile revealed from SAXS measurements (at. % = atomic %). (B) Cyclic voltammetry in a designated potential region (red curve) as compared to the voltammetry obtained from the Pt(111) surface (blue curve). (C) Surface coverage calculated from cyclic voltammograms of $Pt_3Ni(111)$ (red curve) and Pt(111) (blue curve); polarization curves obtained from RRDE measurements. θ_{oxide}, surface coverage by adsorbed spectator oxygenated species. (D) Green scale refering to hydrogen peroxide production in a designated potential region. (E) ORR currents measured on $Pt_3Ni(111)$ (red curve), Pt(111) (blue curve), and polycrystalline platinum (Pt poly; gray curve) surfaces. The arrows are showing the positive potential shift of 100 mV in the electrode half-potential ($\Delta E_{1/2}$) between ORR polarization curves measured on Pt poly and $Pt_3Ni(111)$ surfaces. I, II, and III represent potential regions of H_{upd} adsorption/desorption processes, double-layer region, and region of OH_{ad} layer formation, respectively.[48]

(69) Lim, B.; Jiang, M. J.; Camargo, P. H. C.; Cho, E. C.; Tao, J.; Lu, X. M.; Zhu, Y. M.; Xia, Y. A. *Science* **2009**, *324*, 1302–1305.
(70) Peng, Z. M.; Yang, H. *J. Am. Chem. Soc.* **2009**, *131*, 7542–.
(71) Zhang, J.; Sasaki, K.; Sutter, E.; Adzic, R. R. *Science* **2007**, *315*, 220–222.
(72) Stamenkovic, V. R.; Mun, B. S.; Arenz, M.; Mayrhofer, K. J. J.; Lucas, C. A.; Wang, G.; Ross, P. N.; Markovic, N. M. *Nat. Mater.* **2007**, *6*, 241–247.
(73) Adzic, R.; Zhang, J.; Sasaki, K.; Vukmirovic, M.; Shao, M.; Wang, J.; Nilekar, A.; Mavrikakis, M.; Valerio, J.; Uribe, F. *Top. Catal.* **2007**, *46*, 249–262.
(74) Zhang, J.; Mo, Y.; Vukmirovic, M. B.; Klie, R.; Sasaki, K.; Adzic, R. R. *J. Phys. Chem. B* **2004**, *108*, 10955–10964.

in these cases, the platinum has been replaced by another noble metal so the improvements in cost are not as high as might be achieved in alloys with base metals.

The noble metal content in ORR catalysts can be reduced by utilizing carbon-supported nanoparticles with non-noble metal cores and noble metal shells.[73] One notable example has employed this technique to form a platinum monolayer on carbon-supported Co@Pd core−shell nanoparticles with 3−4 nm diameters exhibiting total noble metal mass activities of 0.4 A/mg at 0.9 V_{RHE}, which is very close to the target for automotive applications.[77] Further investigations are needed to determine the long-term durability of these particles; also the preparation is complex and may not be amenable to large-scale production.

A third highly successful method for producing platinum alloy nanoparticles with platinum-enriched surface layers is electrochemical dealloying.[78−82] In this technique, precursor particles containing platinum and the base metal (copper or cobalt) are supported on carbon and subjected to several hundred potential cycles, which causes the base metal to leach out of the particles (Figure 7). Once dissolution is complete, a roughened platinum-enriched skin is left coating the alloy particle. In a final step, the electrode is rinsed in an inorganic acid to displace the base metal cations trapped in the ionomer membrane. This procedure is more effective at removing the base metal than acid leaching, so fewer cations leach from the catalyst during operation of the fuel cell. This technique produces catalysts with very high surface areas and high specific activities (attributed to electronic effects), yielding catalysts with exceptionally high platinum mass activities. A $Pt_{20}Cu_{20}Co_{60}$ alloy demonstrated a mass activity of 0.5 A/mg_{Pt} at 0.9 V, exceeding the activity benchmark for practical applications.[80] The durability of these particles was found to be similar to that of Pt/C.

Non-Platinum Alloys. The ORR activity of a variety of palladium and palladium alloy nanoparticles has been investigated and is generally lower than that observed for platinum.[41,83−92] While palladium is about one-fifth as expensive as platinum, these savings are offset by the reduced efficiency and increased costs of other materials needed for larger electrode areas. These materials are more likely to find use in direct methanol fuel cells because palladium is more tolerant of methanol than platinum. Several reports have claimed activity comparable to that of platinum on the basis of voltammetry; however, the actual activities at 0.9 V_{RHE} were not reported.[93−96]

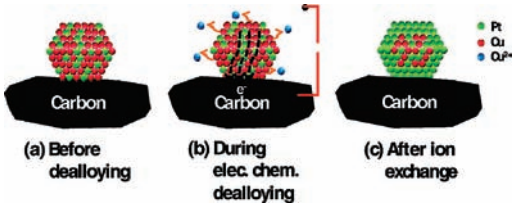

Figure 7. Illustration of the stepwise in situ preparation of dealloyed Pt−Cu electrocatalysts by voltammetric selective dissolution of copper from a $Pt_{25}Cu_{75}$ precursor catalyst. (a) Carbon-supported $Pt_{25}Cu_{75}$ precursor at a MEA cathode. (b) Electrochemical dissolution of Cu atoms from a precursor by cyclic voltammetry. (c) Formation of a platinum-enriched core−shell nanoparticle catalyst with surrounding Cu ions removed by ion exchange.[78]

4. Metalloporphyrins and Pyrolyzed Materials

While precious metal catalysts are presently the most active materials for the ORR, their utility is limited by cost and stability considerations for the activity they present. Consequently, there are substantial efforts directed at developing nonprecious metal (NPM)-based ORR catalysts. This area has recently been reviewed.[97]

An early discovery by Jasinski that cobalt phthalocyanine catalyzed the ORR[98,99] was the basis for considerable subsequent work. Noteworthy among these were the bis-cofacial cobalt porphyrins made by Collman and Anson, which exhibited higher activity relative to the early phthalocyanines.[100−105] More recently, work with molecular systems

(75) Zhang, J.; Lima, F. H. B.; Shao, M. H.; Sasaki, K.; Wang, J. X.; Hanson, J.; Adzic, R. R. *J. Phys. Chem. B* **2005**, *109*, 22701–22704.
(76) Zhang, J.; Vukmirovic, M. B.; Sasaki, K.; Nilekar, A. U.; Mavrikakis, M.; Adzic, R. R. *J. Am. Chem. Soc.* **2005**, *127*, 12480–12481.
(77) Shao, M.; Sasaki, K.; Marinkovic, N. S.; Zhang, L.; Adzic, R. R. *Electrochem. Commun.* **2007**, *9*, 2848–2853.
(78) Mani, P.; Srivastava, R.; Strasser, P. *J. Phys. Chem. C* **2008**, *112*, 2770–2778.
(79) Koh, S.; Strasser, P. *J. Am. Chem. Soc.* **2007**, *129*, 12624–12625.
(80) Srivastava, R.; Mani, P.; Hahn, N.; Strasser, P. *Angew. Chem., Int. Ed.* **2007**, *46*, 8988–8991.
(81) Liu, Z.; Koh, S.; Yu, C.; Strasser, P. *J. Electrochem. Soc.* **2007**, *154*, B1192–B1199.
(82) Schulenburg, H.; Muller, E.; Khelashvili, G.; Roser, T.; Bonnemann, H.; Wokaun, A.; Scherer, G. G. *J. Phys. Chem. C* **2009**, *113*, 4069–4077.
(83) Xiao, L.; Zhuang, L.; Liu, Y.; Lu, J. T.; Abruna, H. D. *J. Am. Chem. Soc.* **2009**, *131*, 602–608.
(84) Shao, M.; Liu, P.; Zhang, J.; Adzic, R. *J. Phys. Chem. B* **2007**, *111*, 6772–6775.
(85) Fernandez, J. L.; Walsh, D. A.; Bard, A. J. *J. Am. Chem. Soc.* **2004**, *127*, 357–365.
(86) Liu, H.; Li, W.; Manthiram, A. *Appl. Catal., B* **2009**, *90*, 184–194.
(87) Majumdar, A.; Pal, K.; Sarkar, S. *Inorg. Chem.* **2008**, *47*, 3393–3401.
(88) Wang, X. P.; Kariuki, N.; Vaughey, J. T.; Goodpaster, J.; Kumar, R.; Myers, D. J. *J. Electrochem. Soc.* **2008**, *155*, B602–B609.
(89) Tominaka, S.; Momma, T.; Osaka, T. *Electrochim. Acta* **2008**, *53*, 4679–4686.
(90) Wang, W. M.; Zheng, D.; Du, C.; Zou, Z. Q.; Zhang, X. G.; Xia, B. J.; Yang, H.; Akins, D. L. *J. Power Sources* **2007**, *167*, 243–249.
(91) Mustain, W. E.; Kepler, K.; Prakash, J. *Electrochim. Acta* **2007**, *52*, 2102–2108.
(92) Savadogo, O.; Lee, K.; Oishi, K.; Mitsushima, S.; Kamiya, N.; Ota, K. I. *Electrochem. Commun.* **2004**, *6*, 105–109.
(93) Raghuveer, V.; Ferreira, P. J.; Manthiram, A. *Electrochem. Commun.* **2006**, *8*, 807–814.
(94) Fernandez, J. L.; Raghuveer, V.; Manthiram, A.; Bard, A. J. *J. Am. Chem. Soc.* **2005**, *127*, 13100–13101.
(95) Raghuveer, V.; Manthiram, A.; Bard, A. J. *J. Phys. Chem. B* **2005**, *109*, 22909–22912.
(96) Shao, M.-H.; Sasaki, K.; Adzic, R. R. *J. Am. Chem. Soc.* **2006**, *128*, 3526–3527.
(97) Scherson, D. A.; Palencsar, A.; Tolmachev, Y.; Stefan, I. *Adv. Electrochem. Sci. Eng.* **2008**, *10*, 191–288.
(98) Jasinski, R. J. *J. Electrochem. Soc.* **1965**, *112*, 526–528.
(99) Jasinski, R. J. *Nature* **1964**, *201*, 1212–1213.
(100) Collman, J. P.; Marrocco, M.; Denisevich, P.; Koval, C.; Anson, F. C. *J. Electroanal. Chem. Interfacial Electrochem.* **1979**, *101*, 117–122.
(101) Collman, J. P.; Anson, F. C.; Barnes, C. E.; Bencosme, C. S.; Geiger, T.; Evitt, E. R.; Kreh, R. P.; Meier, K.; Pettman, R. B. *J. Am. Chem. Soc.* **1983**, *105*, 2694–2699.
(102) Durand, R. R., Jr.; Bencosme, C. S.; Collman, J. P.; Anson, F. C. *J. Am. Chem. Soc.* **1983**, *105*, 2710–2718.
(103) Collman, J. P.; Anson, F. C.; Bencosme, S.; Chong, A.; Collins, T.; Denisevich, P.; Evitt, E.; Geiger, T.; Ibers, J. A.; et al. *Org. Synth.: Today Tomorrow, Proc. IUPAC Symp. Org. Synth., 3rd* **1981**, 29–45.
(104) Collman, J. P.; Denisevich, P.; Konai, Y.; Marrocco, M.; Koval, C.; Anson, F. C. *J. Am. Chem. Soc.* **1980**, *102*, 6027–6036.
(105) Shi, C.; Anson, F. C. *Inorg. Chem.* **1990**, *29*, 4298–4305.

has extended to the so-called "pac-man" porphyrins,[106,107] which feature two porphyrins attached to each other via a flexible tether, enabling the design of catalysts with tunable metal−metal separations. A typical preparation of these materials features synthesis of the candidate material and then their subsequent adsorption onto a carbon scaffold. The most successful material in this regard has been edge-plane graphite, although other carbons work to a lesser extent. The effort examining the ORR activity of adsorbed porphyrins and related compounds continues to the present day.[108,109]

Three issues remain outstanding with these adsorbed porphyrinic materials relative to their use as ORR catalysts. First, the overall activity of the NPM catalysts is low, with onset potentials around +600 mV vs RHE. This is some 500−600 mV lower than desired. Second, the materials are not stable to long-term use in a MEA. Third, from mechanistic and synthetic points of view, a major issue with these systems is the lack of activity found when using supports other than edge-plane graphite (such as Au, MoS_2, or even basal-plane highly oriented pyrolytic graphite). Yeager suggested over 25 years ago that the porphyrin was decomposed by functionality on the graphite edge plane.[110,111]

Definitive characterization of the state of the material after adsorption on edge-plane graphite has not yet been forthcoming, and demonstrations that the active material is, in fact, an intact porphyrin are lacking. A demonstration of substantial activity on a different support, or a more detailed characterization of the active site, would revive confidence that the molecular species is, in fact, intact on the electrode surface. However, the observation that the pyrolysis product is as active as the molecular species (vide infra) casts substantial doubt regarding the on-electrode integrity of the porphyrinic materials synthesized to date.

As early as 1983, there were suggestions that pyrolyzed cobalt porphyrins could also function as ORR catalysts.[112] Additionally, Yeager and co-workers showed that an active catalyst could be synthesized starting from nitrogen and cobalt precursors rather than the porphyrinic materials.[113,114] By the early 1990s, Dodelet and co-workers showed that pyrolyzed cobalt porphyrins exhibit reactivity equal to or greater than the intact species,[115] in de facto confirmation of Yeager's original supposition. Spectroscopic methods suggested that pyrolysis resulted in the formation of cobalt clusters, which were then postulated as the active site.[116] More recently, both the Dodelet and Dahn groups have optimized the materials obtained starting from elemental iron and/or cobalt, and a nitrogen source pyrolyzed on carbon at temperatures between 700 and 1000 °C depending on the conditions, and shown that activities much greater than those found with cobalt porphyrins could be obtained. A combinatoric approach yielded improved materials.[117] A recent report described an optimized synthesis of these materials exhibiting activities very close to those requested in the DOE roadmap[118] but still with durability at least 2 orders of magnitude less than needed.

There are several unanswered questions regarding the pyrolyzed materials, the most important of which relate to the structure of the active site and the fairly poor stability attendant their use. The most recent understanding of the active site structure features Fe or Co cations coordinated in some way by pyridinic N atom functionalities in the interstices of graphitic carbon sheets.[118−120] However, there is no detailed coordination picture yet available concerning the structure of the active site or its evolution with oxygen coordination. This lack severely limits both the understanding and the search for new catalyst materials. Additionally, there is relatively little understanding regarding the decomposition pathways(s) of the pyrolyzed species. Nonetheless, at present, these materials are the most active synthetic NPM catalysts for the ORR, and this alone certainly justifies substantial continuing effort on these systems.

5. Carbons

The observation that pyrolysis of carbon in the presence of nitrogen and a transition metal leads to an ORR catalyst has prompted some researchers to suggest that the role of the transition metal is merely to promote insertion of nitrogen into defects in the carbon lattice. These defects might promote the generation of pyridinic N centers, which are thought to be good ORR catalysts in their own right.[121] Substantial recent progress in this area has shown four-electron reduction of oxygen in acid at fairly large overpotentials,[122−126] with considerably better results in base. Indeed, a recent report showed that a modified carbon could also effect four-electron ORR again in the basic electrochemical environment.[127]

(106) Chang, C. J.; Baker, E. A.; Pistorio, B. J.; Deng, Y. Q.; Loh, Z. H.; Miller, S. E.; Carpenter, S. D.; Nocera, D. G. *Inorg. Chem.* **2002**, *41*, 3102–3109.
(107) Chang, C. J.; Deng, Y. Q.; Shi, C. N.; Chang, C. K.; Anson, F. C.; Nocera, D. G. *Chem. Commun.* **2000**, 1355–1356.
(108) Okunola, A.; Kowalewska, B.; Bron, M.; Kulesza, P. J.; Schuhmann, W. *Electrochim. Acta* **2009**, *54*, 1954–1960.
(109) Elbaz, L.; Korin, E.; Soifer, L.; Bettelheim, A. *J. Electroanal. Chem.* **2008**, *621*, 91–96.
(110) Scherson, D. A.; Yao, S. B.; Yeager, E. B.; Eldridge, J.; Kordesch, M. E.; Hoffman, R. W. *J. Phys. Chem.* **1983**, *87*, 932–943.
(111) Simic-Glavaski, B.; Zecevic, S.; Yeager, E. *J. Electroanal. Chem. Interfacial Electrochem.* **1983**, *150*, 469–479.
(112) Scherson, D. A.; Gupta, S. L.; Fierro, C.; Yeager, E. B.; Kordesch, M. E.; Eldridge, J.; Hoffman, R. W.; Blue, J. *Electrochim. Acta* **1983**, *28*, 1205–1209.
(113) Gupta, S. L.; Tryk, D.; Daroux, M.; Aldred, W.; Yeager, E. *Proc. Electrochem. Soc.* **1986**, *86−10*, 207–218.
(114) Scherson, D.; Tanaka, A. A.; Gupta, S. L.; Tryk, D.; Fierro, C.; Holze, R.; Yeager, E. B.; Lattimer, R. P. *Electrochim. Acta* **1986**, *31*, 1247–1258.
(115) Ladouceur, M.; Lalande, G.; Guay, D.; Dodelet, J. P.; Dignardbailey, L.; Trudeau, M. L.; Schulz, R. *J. Electrochem. Soc.* **1993**, *140*, 1974–1981.
(116) Dignardbailey, L.; Trudeau, M. L.; Joly, A.; Schulz, R.; Lalande, G.; Guay, D.; Dodelet, J. P. *J. Mater. Res.* **1994**, *9*, 3203–3209.
(117) Yang, R. Z.; Bonakdarpour, A.; Easton, E. B.; Stoffyn-Egli, P.; Dahn, J. R. *J. Electrochem. Soc.* **2007**, *154*, A275–A282.
(118) Lefevre, M.; Proietti, E.; Jaouen, F.; Dodelet, J. P. *Science* **2009**, *324*, 71–74.
(119) Matter, P. H.; Zhang, L.; Ozkan, U. S. *J. Catal.* **2006**, *239*, 83–96.
(120) Herranz, J.; Lefevre, M.; Dodelet, J. P. *J. Electrochem. Soc.* **2009**, *156*, B593–B601.
(121) Wang, P.; Ma, Z. Y.; Zhao, Z. C.; Ha, L. X. *J. Electroanal. Chem.* **2007**, *611*, 87–95.
(122) Biddinger, E. J.; von Deak, D.; Ozkan, U. S. *Top. Catal.* **2009**, *52*, 1566–1574.
(123) Matter, P. H.; Wang, E.; Millet, J. M. M.; Ozkan, U. S. *J. Phys. Chem. C* **2007**, *111*, 1444–1450.
(124) Matter, P. H.; Wang, E.; Arias, M.; Biddinger, E. J.; Ozkan, U. S. *J. Mol. Catal A: Chem.* **2007**, *264*, 73–81.
(125) Matter, P. H.; Wang, E.; Ozkan, U. S. *J. Catal.* **2006**, *243*, 395–403.
(126) Subramanian, N. P.; Li, X. G.; Nallathambi, V.; Kumaraguru, S. P.; Colon-Mercado, H.; Wu, G.; Lee, J. W.; Popov, B. N. *J. Power Sources* **2009**, *188*, 38–44.
(127) Gong, K. P.; Du, F.; Xia, Z. H.; Durstock, M.; Dai, L. M. *Science* **2009**, *323*, 760–764.

A high activity for the ORR in acid has yet to be achieved, however, with a metal-free catalyst.

Carbon in a basic solution is an efficient catalyst for the two-electron reduction of oxygen to peroxide.[128,129] In the zinc/air battery, the peroxide then disproportionates in the presence of a MnO_2 catalyst to make water and dioxygen. Incorporating this disproportionation idea into an acid-stable catalyst could in concept provide a high activity and is a focus of research.

6. Metal Chalcogenides

An important class of ORR catalysts are formed by the metal chalcogenides. In the mid-1990s, Alonsovante and co-workers reported a Re_xSe_y material that exhibited four-electron oxygen reduction at modest (ca. 500 mV) overpotentials in acid.[130−132] Investigation reveals a large series of sulfides and selenides exhibiting this activity, with some of the best examples formed from Fe_xSe_y and Co_xSe_y. These materials have several advantages. First, they do not feature precious metals and so are intrinsically less expensive relative to the platinum-based catalysts. Second, they are methanol-tolerant, which could be a considerable advantage in direct methanol fuel cells, where the methanol fuel can cross over the membrane and react at the cathode; this reactivity can substantially depolarize platinum-catalyst-based cells. To this list must be added disadvantages. Most prominently, the selenium materials exhibit substantial toxicity, while the sulfides are considerably less active with the best overpotentials in the 400−500 mV range. Additionally, the materials do not feature the stability required for fuel-cell applications.

Studies of the chalcogenide materials suggest that the active phases feature a sulfur- or selenium-rich surface surrounding a metal core. Photoemission spectra suggest that the underlying metal couples electronically with the chalcogenide, while X-ray adsorption studies suggest that M−M interactions are present during the ORR. This result implies that rearrangement of the M−Se cluster occurs during reactivity.[133−135]

7. Enzyme-Modified Electrodes

The highest-activity ORR catalysts are actually found in implementations using laccase, a type of multicopper oxidase enzyme.[136] These enzymes catalyze the oxidation of lignins and utilize dioxygen as the oxidant. The ORR onset potential for laccase-modified electrodes can approach the 1.2 V_{RHE} reversible potential of the O_2/H_2O half-cell; at 0.9 V_{RHE},

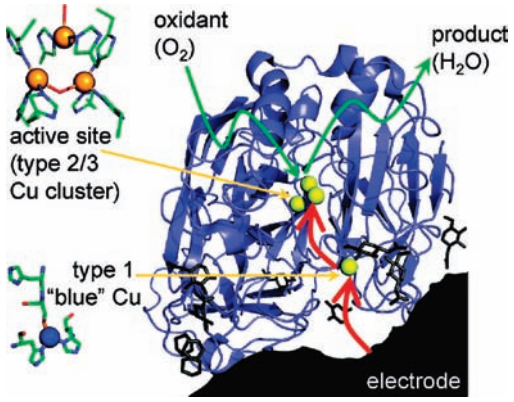

Figure 8. Ribbon representation of the crystal structure of *Trametes versicolor laccase* (PDB code 1KYA; structure solved by Bettelheim et al.[109]) showing the protein superstructure in blue and the Cu atoms as yellow spheres.[138]

where the platinum activity is evaluated, the current is limited by the rate of diffusion of dioxygen to the electrode surface rather than the kinetics of the ORR.[137] The dioxygen molecule is activated at a three-Cu active site (Figure 8), and the substrate is oxidized remotely at a separate one-Cu site.[138] This spatial separation between dioxygen activation and substrate oxidation makes these enzymes particularly amenable to application as electrocatalysts upon establishing electron transfer with an electrode surface in lieu of substrate oxidation.[139] Two general strategies have been employed to attach the enzyme to the electrode surface and establish electronic communication. The first utilizes an electron-transfer mediator, typically an osmium complex, to shuttle electrons between the enzyme and the electrode surface.[137,140−147] This method allows thick layers of enzyme to be used, leading to good durability and larger current denisities; however, the potential of the electrode is determined by the mediator. Direct electron transfer between laccase and carbon electrodes can also be established by utilizing a diazonium coupling reaction to modify the electrode surface with polycyclic aromatic molecules (such as anthracene).[139,148] These aromatic molecules facilitate binding of laccase to the electrode in a favorable orientation and assist in electron transfer to the active site. Direct electron transfer eliminates the need for a mediator so the electrode activity is determined by the

(128) Zhu, W. H.; Poole, B. A.; Cahela, D. R.; Tatarchuk, B. J. *J. Appl. Electrochem.* **2003**, *33*, 29–36.
(129) Dewi, E. L.; Oyaizu, K.; Nishide, H.; Tsuchida, E. *J. Power Sources* **2004**, *130*, 286–290.
(130) Solorzaferia, O.; Ellmer, K.; Giersig, M.; Alonsovante, N. *Electrochim. Acta* **1994**, *39*, 1647–1653.
(131) Alonsovante, N.; Tributsch, H.; Solorzaferia, O. *Electrochim. Acta* **1995**, *40*, 567–576.
(132) Kochubey, D. I.; Nikitenko, S. G.; Parmon, V. N.; Gruzdkov, Y. A.; Tributsch, H.; Alonsovante, N. *Physica B* **1995**, *209*, 694–696.
(133) Ziegelbauer, J. M.; Gatewood, D.; Gulla, A. F.; Guinel, M. J. F.; Ernst, F.; Ramaker, D. E.; Mukerjee, S. *J. Phys. Chem. C* **2009**, *113*, 6955–6968.
(134) Ziegelbauer, J. M.; Murthi, V. S.; O'Laoire, C.; Guila, A. F.; Mukerjee, S. *Electrochim. Acta* **2008**, *53*, 5587–5596.
(135) Ziegelbauer, J. M.; Gatewood, D.; Gulla, A. F.; Ramaker, D. E.; Mukerjee, S. *Electrochem. Solid State Lett.* **2006**, *9*, A430–A434.
(136) Solomon, E. I.; Sundaram, U. M.; Machonkin, T. E. *Chem. Rev.* **1996**, *96*, 2563–2605.
(137) Mano, N.; Soukharev, V.; Heller, A. *J. Phys. Chem. B* **2006**, *110*, 11180–11187.
(138) Cracknell, J. A.; Vincent, K. A.; Armstrong, F. A. *Chem. Rev.* **2008**, *108*, 2439–2461.
(139) Blanford, C. F.; Foster, C. E.; Heath, R. S.; Armstrong, F. A. *Faraday Discuss.* **2009**, *140*, 319–335.
(140) Gallaway, J. W.; Calabrese Barton, S. A. *J. Am. Chem. Soc.* **2008**, *130*, 8527–8536.
(141) Hudak, N. S.; Gallaway, J. W.; Barton, S. C. *J. Electrochem. Soc.* **2009**, *156*, B9–B15.
(142) Hudak, N. S.; Gallaway, J. W.; Barton, S. C. *J. Electroanal. Chem.* **2009**, *629*, 57–62.
(143) Gallaway, J.; Wheeldon, I.; Rincon, R.; Atanassov, P.; Banta, S.; Barton, S. C. *Biosens. Bioelectron.* **2008**, *23*, 1229–1235.
(144) Soukharev, V.; Mano, N.; Heller, A. *J. Am. Chem. Soc.* **2004**, *126*, 8368–8369.
(145) Barton, S. C.; Pickard, M.; Vazquez-Duhalt, R.; Heller, A. *Biosens. Bioelectron.* **2002**, *17*, 1071–1074.
(146) Barton, S. C.; Kim, H. H.; Binyamin, G.; Zhang, Y. C.; Heller, A. *J. Am. Chem. Soc.* **2001**, *123*, 5802–5803.
(147) Barton, S. C.; Kim, H. H.; Binyamin, G.; Zhang, Y. C.; Heller, A. *J. Phys. Chem. B* **2001**, *105*, 11917–11921.
(148) Blanford, C. F.; Heath, R. S.; Armstrong, F. A. *Chem. Commun.* **2007**, 1710–1712.

enzyme; however, the thin films of enzyme are less durable and support relatively lower current densities than mediated electrodes.[138] In spite of their activity at remarkably high potential, there are significant barriers to the practical use of enzyme-modified electrodes including high cost, limited durability, limited pH ranges (4−7), and low power densities because of low surface coverage.[149,150]

8. Coordination Polymers and Transition-Metal Complexes

A final strategy in the search for noble metal free electrocatalysts is the use of insoluble transition-metal complexes including coordination polymers and complexes with coordinating polymers.[151−157] The insolubility is necessary to prevent dissolution of the metal at the high potentials typically utilized during the ORR. Coordination polymers are more durable than the base metals and soluble complexes, which can corrode or desorb from the electrode, and better defined than materials prepared by pyrolysis. Indeed, the coordination polymer formed by copper(I) and benzotriazole is often utilized to inhibit copper metallic corrosion in many different contexts.[158−160]

Initial work examining coordination polymer ORR catalyts investigated the complexes formed between transition metals and a coordinating polymer backbone, such as polypyrrole.[151,154−157] The most notable example is a carbon-supported cobalt polypyrrole composite material that has an ORR onset at ca. 0.7 V_{RHE} and shows no degradation during 100 h lifetime studies.[157] However, there is still little known about the exact nature of the active site in this material.[6]

Recently, our group has focused on evaluating the activity of insoluble coordination complexes. The high ORR activity of laccase led us to investigate the ORR activity of copper complexes coordinated with bridging azole-type ligands because these might provide stability in addition to multicopper sites to bind and activate dioxygen. The combination of aqueous solutions of $CuSO_4$ with a variety of substituted pyrazole and triazole ligands leads to the precipitation of insoluble compounds (Figure 9). Direct precipitation of these compounds onto carbon black suspended in the reaction mixture provides a simple method to incorporate these materials into existing electrode fabrication methods. This simple method also allows utilization of the characterization techniques developed for carbon-supported platinum catalysts. Finally, the use of a carbon black support could facilitate the transition to practical application upon the discovery of a suitable catalyst.

Figure 9. Model of the ORR site on the copper dimer formed by a substituted triazole. Reprinted with permission from ref 152. Copyright Wiley-VCH 2009.

The carbon-supported complex of copper(II) and 3,5-diamino-1,2,4-triazole was found to be an active catalyst with an ORR onset ranging from 0.5 V_{RHE} (pH 1) to 0.8 V_{RHE} (pH 13) and good durability at intermediate pHs. This material is the most active synthetic copper-based ORR catalyst reported to date, and for the first time, we applied magnetic susceptibility measurements to prove the presence of multiple-Cu sites on the electrode surface. Most importantly, the viability of this approach opens the door to the evaluation of the ORR activity of a wide variety of insoluble coordination complexes that have hitherto been overlooked; the high activity of laccase proves that it should be possible to prepare a highly active material based on first-row transition-metal complexes that is more active than platinum.

9. Conclusions

The intent of this short and certainly less than comprehensive review is to give readers some of the flavor of research into the ORR and to explain its importance. It is likely that pure platinum nanoparticle catalysts will be unable to meet the ORR activity and durability requirements for large-scale fuel-cell applications. However, the combination of platinum with other metals in the form of alloys or heterogeneous nanostructures allows significant enhancements in the activity and/or durability, although no material currently meets both activity and durability requirements simultaneously. These advancements have enabled significant reductions in the platinum loading; however, present day reductions in the ORR overpotential are relatively minor (on the order of tens of millivolts) and, consequently, the challenge of fuel-cell thermodynamic efficiency remains.

Nonetheless, platinum-based nanoparticle catalysts remain the most active materials known to date for the ORR outside of the biological materials operating at room temperature and neutral pHs. The existence of the biological materials functions as proof that an all-inorganic, NPM solution for the ORR does exist, although stabilizing any putative catalyst in the acid electrochemical environment at high potentials will undoubtedly be a challenge. The challenge for inorganic and coordination chemists is to translate the activity of the biological materials into a robust fuel-cell solution. Undoubtedly, this will form a focus of future research.

Acknowledgment. This work was funded by the U.S. Department of Energy (Contract DE-FG02-87ER46260), which is gratefully acknowledged.

(149) Barton, S. C.; Gallaway, J.; Atanassov, P. *Chem. Rev.* **2004**, *104*, 4867–4886.
(150) *Faraday Discuss.* **2009**, *140*, 417−437.
(151) Weng, Y. C.; Fan, F. R. F.; Bard, A. J. *J. Am. Chem. Soc.* **2005**, *127*, 17576–17577.
(152) Thorum, M. S.; Yadav, J.; Gewirth, A. A. *Angew. Chem., Int. Ed.* **2009**, *48*, 165–167.
(153) Kim, J.; Gewirth, A. A. *Bull. Korean Chem. Soc.* **2007**, *28*, 1322–1328.
(154) Yuasa, M.; Yamaguchi, A.; Itsuki, H.; Tanaka, K.; Yamamoto, M.; Oyaizu, K. *Chem. Mater.* **2005**, *17*, 4278–4281.
(155) Millan, W. M.; Smit, M. A. *J. Appl. Polym. Sci.* **2009**, *112*, 2959–2967.
(156) Lee, K.; Zhang, L.; Lui, H.; Hui, R.; Shi, Z.; Zhang, J. J. *Electrochim. Acta* **2009**, *54*, 4704–4711.
(157) Bashyam, R.; Zelenay, P. *Nature* **2006**, *443*, 63–66.
(158) Poling, G. W. *Corros. Sci.* **1970**, *10*, 359–370.
(159) Leung, T. Y. B.; Kang, M. C.; Corry, B. F.; Gewirth, A. A. *J. Electrochem. Soc.* **2000**, *147*, 3326–3337.
(160) Schultz, Z. D.; Biggin, M. E.; White, J. O.; Gewirth, A. A. *Anal. Chem.* **2004**, *76*, 604–609.